Arch. Min. Sci. **63** (2018), 1, 3-26

Electronic version (in color) of this paper is available: http://mining.archives.pl

DOI 10.24425/118882

MAREK PŁACHNO*#

MATHEMATICAL MODEL OF TRANSVERSE VIBRATIONS OF A HIGH-CAPACITY MINING SKIP DUE MISALIGNMENT OF THE GUIDING TRACKS IN THE HOISTING SHAFT

MODEL MATEMATYCZNY DRGAŃ POPRZECZNYCH SKIPU GÓRNICZEGO O DUŻEJ ŁADOWNOŚCI POWODOWANYCH PRZEZ NIERÓWNOŚCI TORÓW PROWADZENIA TEGO SKIPU W SZYBIE

A solution is suggested to the problem which has received a great deal of researchers' attention in the last twenty years involving the development of a mathematical model of transverse vibration experienced by high-capacity mining skips while they traverse the shaft. Such model, particularly useful when investigating fatigue damage of hoisting skips, is still being sought by engineering practitioners responsible for hoist safety. Models proposed so far have been found unsatisfactory, which was corroborated by research data showing that the underlying assumptions and involved equations need to be modified. This paper highlights the suggested modifications, basing on measurement data and the modified version of the model is verified against those data.

Keywords: mining skips, misalignment of the guiding tracks, transverse vibration, mathematical model

W artykule zaproponowano rozwiązanie problemu naukowego, jakim od ponad dwudziestu lat jest model matematyczny drgań poprzecznych doznawanych przez skipy górnicze o dużych ładownościach podczas jazdy w szybach. Taki model, przydatny w szczególności do opracowania metody obliczeń dla zmęczeniowej trwałości skipów projektowanych, jest oczekiwany przez środowisko inżynierskie odpowiedzialne za bezpieczeństwo wyciągów górniczych. Obliczenia trwałości jw. nie są, jak dotąd, wykonywane, wskutek czego znacząca część skipów mających duże ładowności – aktualnie użytkowanych – doznaje uszkodzeń zmęczeniowych po wykonaniu w szybie znacznie mniej cykli transportowych niż zaplanowano. W artykule podano wyniki badań (Rys. 5) drgań poprzecznych takich skipów wykazujące, że opublikowane dotychczas propozycje przedmiotowego modelu są niekompletne i wymagają aktualizacji zarówno co do założeń jak i jego równań. W artykule zaproponowano taką aktualizację opartą o zamieszczone wyniki badań, a także sformułowano nową propozycję omawianego modelu (6)÷(32), zweryfikowaną w oparciu o te wyniki.

Słowa kluczowe: skipy górnicze, nierówności torów prowadzenia w szybie, drgania poprzeczne, model matematyczny

* AGH UNIVERSITY OF SCIENCE AND TECHNOLOGY, FACULTY OF MECHANICAL ENGINEERING AND ROBOTICS, AL. MICKIEWICZA 30, 30-059 KRAKÓW, POLAND

\# Corresponding author: plachno@agh.edu.pl

1. Introduction

A typical design structure of high-capacity mining skips (Fig. 1) incorporates three main mass components: the skip head, the hopper and the bottom frame, supported by vertical rods (external and middle), also referred to as pull rods.

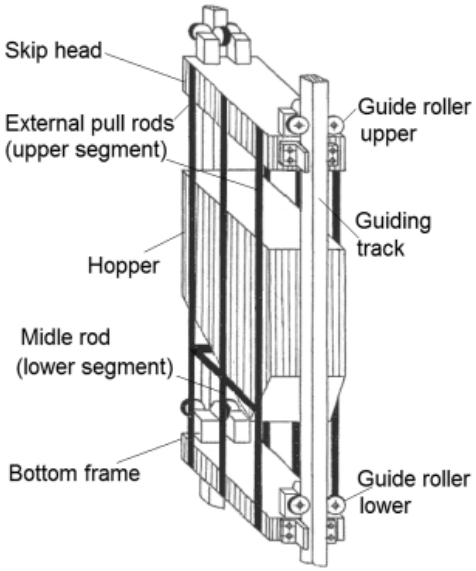

Fig. 1. Design structure of high-capacity mining skip

Presently such high-capacity skips are widely operated in mine shafts and as early as in the 1960s that design solution was found most successful, ensuring good hoisting efficiency. Load-bearing capacity of largest skips for hoisting coal approaches 40 Mg, whilst the skips for hauling ores have the capacity over 50 Mg.

In the early 1980s, soon after high-capacity skips came into widespread use, maintenance engineers registered the fatigue damage to load-bearing pull rods after a smaller number of duty cycles than planned (Kędziora, 1983; Płachno et al., 1984-1989; Fuchs & Noeller, 1988). This kind of damage was found to pose a major hazard to hoisting installations, at the same time jeopardising the mine production schedules. Extensive research efforts were made, therefore, to diagnose the problem and specialist teams were formed responsible for regular inspection of pull rods for defects (Brodziński & Śmiałek, 1993) and for corrective maintenance in case when such faults were detected (Bąk & Myszor, 1999).

Researchers involved in the mining sector, including Polish engineers, thoroughly investigated and diagnosed the problem before 1980s, which is evidenced by numerous publications (Płachno, 1988; Fuchs & Noeller, 1988), demonstrating that the fatigue damage is induced by variations of stresses acting in pull rods caused by enhanced levels of transverse vibration of the skip hopper whose mass is much larger than that of the two remaining skip components. It turned out that variable loads acting upon the pull rods are much larger in high-capacity than in

low-capacity skips, which results in a significant increase of variable stresses in pull rods, out of proportion to the load-bearing capacity of the skip.

These investigations finally established that the problem was caused by random irregularities and misalignment of the guiding tracks in the shaft, giving rise to varied – amplitude dynamic forces in roller guides and inducing random transverse vibration of the skip. These findings prompted further research efforts to develop a mathematical model of these vibrations enabling the problem to be solved by modifying the engineering design of the skip.

Accordingly, research work in Poland was undertaken by three research teams: that headed by the Author (Płachno, 1989, 1999a, 1999b, 2007; Płachno & Rosner, 1997) who continued earlier investigations (Płachno et al., 1984-1989), by Tejszerska and her team (Tejszerska, 1993, 1995, 2002; Tejszerska et al., 2001) and a group of researchers `headed by S. Wolny (Wolny & Bella, 2005; Wolny, 2009; Wolny & Matachowski, 2010, 2011; Matachowski, 2011).

Nevertheless, mathematical models governing the skip's transverse vibration proposed so far were found unsatisfactory by engineers responsible for safety of hoisting installations, because they did not allow the skip fatigue damage to be handled by way of finding an engineering solution to the problem. This assessment was corroborated by research data quoted below, showing that the underlying assumptions and model objectives, certain integral equations and involved relationships need to be modified accordingly.

2. Modified assumptions underlying the equations expressing the skip′s transverse vibration

The modifications are prompted by research data collected by (Płachno et al. 2007-2015) investigating transverse vibration experienced by skips whose load-bearing pull rods were fatigue-damaged and repaired, having completed a lower number of duty cycles than planned. Eight skips were investigated: two with the load-bearing capacity 18 Mg, two skips of 23 Mg and four skips having the capacity 33 Mg. Measurements were taken of the skips' transverse vibration using the specialist equipment (Płachno, 2007) installed to each time in the skip's structure, as shown in the diagram in Fig. 2a and 2b.

Fig. 3. (photo) shows the measuring equipment mounted in the investigated skips: the main unit and an external unit.

As a part of the measurement procedure, each of the four external unit incorporating acceleration transducers was fixed to the main unit for the duration of the measurement. Apart from acceleration transducers, the main unit incorporates the supply system powering the two units and a digital recorder handling its all measurement paths. During each measurement procedure this recorder was synchronised, via a cable (Fig. 2) with the recorder in the second unit and, therefore, each sub-sequently registered acceleration of control points at the top G1g, G2g, D1g, D2g, or at the bottom G1d, G2d, D1d, D2d represented the same time instant.

The test runs being completed and the measuring equipment being removed from the investigated skip, thus registered signals were subsequently transferred by electronic means to the exter-nal computer memory, where they were converted into frequency vs power spectral density patterns and the plots of relative displacements between the test points at the top G1g, D1g, G2g, D2g and at the bottom: G1d, D1d, G2d, D2d. For each investigated skip, the conversion procedure used operator formulas given as:

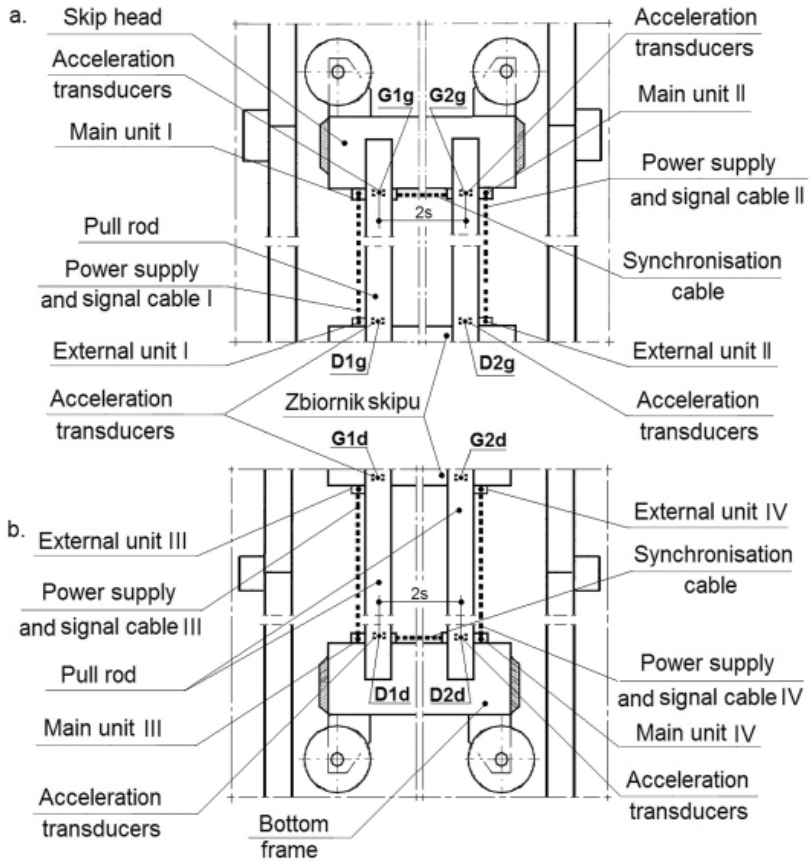

Fig. 2. Equipment (Płachno, 2007) for measuring transverse vibration experienced by the skip head and hopper (Fig 2a) and by the hopper and the bottom frame (Fig. 2b)

Fig. 3. (photo). Main unit (on the left) and external unit (on the right) of the purpose-built system (Płachno, 2007) for measuring skip's transverse vibration while it traverses the shaft

- for control points at the top:

$$u_{bg}(f) = 0{,}5 \cdot \left\{ \left| \frac{FFT\left[b_{D1g}(t)\right]}{4\pi^2 f^2} - \frac{FFT\left[b_{G1g}(t)\right]}{4\pi^2 f^2} \right|^2 + \left| \frac{FFT\left[b_{D2g}(t)\right]}{4\pi^2 f^2} - \frac{FFTb_{G2g}(t)}{4\pi^2 f^2} \right|^2 \right\},$$

$$u_{cg}(f) = 0{,}5 \cdot \left\{ \left| \frac{FFT\left[c_{D1g}(t)\right]}{4\pi^2 f^2} - \frac{FFT\left[c_{G1g}(t)\right]}{4\pi^2 f^2} \right|^2 + \left| \frac{FFT\left[c_{D2g}(t)\right]}{4\pi^2 f^2} - \frac{FFT\left[c_{G2g}(t)\right]}{4\pi^2 f^2} \right|^2 \right\},$$

$$\gamma_{sg}(f) = \left(\frac{1}{s}\right)^2 \cdot \left| \frac{FFT\left[b_{D1g}(t)\right]}{4\pi^2 f^2} + \frac{FFT\left[b_{G2g}(t)\right]}{4\pi^2 f^2} - \frac{FFT\left[b_{G1g}(t)\right]}{4\pi^2 f^2} - \frac{FFT\left[b_{D2g}(t)\right]}{4\pi^2 f^2} \right|^2 \cdot$$

$f \geq 0{,}5\ Hz.$ (1)

- for control points at the bottom:

$$u_{bd}(f) = 0{,}5 \cdot \left\{ \left| \frac{FFT\left[b_{D1d}(t)\right]}{4\pi^2 f^2} - \frac{FFT\left[b_{G1d}(t)\right]}{4\pi^2 f^2} \right|^2 + \left| \frac{FFT\left[b_{D2d}(t)\right]}{4\pi^2 f^2} - \frac{FFT\left[b_{G2d}(t)\right]}{4\pi^2 f^2} \right|^2 \right\},$$

$$u_{cd}(f) = 0{,}5 \cdot \left\{ \left| \frac{FFT\left[c_{D1d}(t)\right]}{4\pi^2 f^2} - \frac{FFT\left[c_{G1d}(t)\right]}{4\pi^2 f^2} \right|^2 + \left| \frac{FFT\left[c_{D2d}(t)\right]}{4\pi^2 f^2} - \frac{FFT\left[c_{G2d}(t)\right]}{4\pi^2 f^2} \right|^2 \right\},$$

$$\gamma_{sd}(f) = \left(\frac{1}{s}\right)^2 \cdot \left| \frac{FFT\left[b_{D1d}(t)\right]}{4\pi^2 f^2} + \frac{FFT\left[b_{G2d}(t)\right]}{4\pi^2 f^2} - \frac{FFT\left[b_{G1d}(t)\right]}{4\pi^2 f^2} - \frac{FFT\left[b_{D2d}(t)\right]}{4\pi^2 f^2} \right|^2 \cdot$$

$f \geq 0{,}5\ Hz.$ (2)

where:

$u_{bg}(f)$, $u_{cg}(f)$, $g_{sg}(f)$ — power spectral densities of relative displacements between the upper control points vs frequency, relative displacements in the lateral motion (in the direction determined by the shorter sides of the skip's main mass components) vs frequency, relative frontal dis-placements (in the direction determined by longer sides of the skip's main mass components) vs frequency and relative displacements in torsion around the vertical axis vs frequency;

$u_{bd}(f)$, $u_{cd}(f)$, $g_{sd}(f)$ — power spectral density patterns of relative displacements between the upper lower points vs frequency: relative displacements in the lateral motion vs frequency, relative frontal displacements vs frequency and relative displacements in torsion around the vertical axis vs frequency;

FFT – Fourier operator transforming the time patterns into the frequency patterns,

$b_{D1g}(t)$, $b_{G1g}(t)$, $b_{D2g}(t)$, $b_{G2g}(t)$, $c_{D1g}(t)$, $c_{D2g}(t)$, $c_{G2g}(t)$ — measured acceleration signals: respective accelerations in lateral and frontal motion registered at control points at the top,

$b_{D1d}(t)$, $b_{G1d}(t)$, $b_{D2d}(t)$, $b_{G2d}(t)$, $c_{D1d}(t)$, $c_{D2d}(t)$, $c_{G2d}(t)$ — measured acceleration signals: respective accelerations in lateral and frontal motion registered at control points at the bottom,

s — dimension indicated in Fig. 2a and 2b.

Accordingly, Eq. (1) and (2) were recalled to obtain two sets of power spectral density patterns of relative displacement for each investigated skip, one set for control points at the top and

one- for control points at the bottom. Each set is assigned three spectral patterns, one associated with relative displacements in lateral motion, one associated with relative frontal displacements and one representing the relative displacements in torsional motion.

As for each investigated skip the plots of corresponding power density patterns were found to be similar in qualitative terms, this study will focus on plots obtained for a 33 Mg skip. They are shown in Fig. 4, the upper section gives the plots obtained for control points at the top, the lower section – for control points at the bottom.

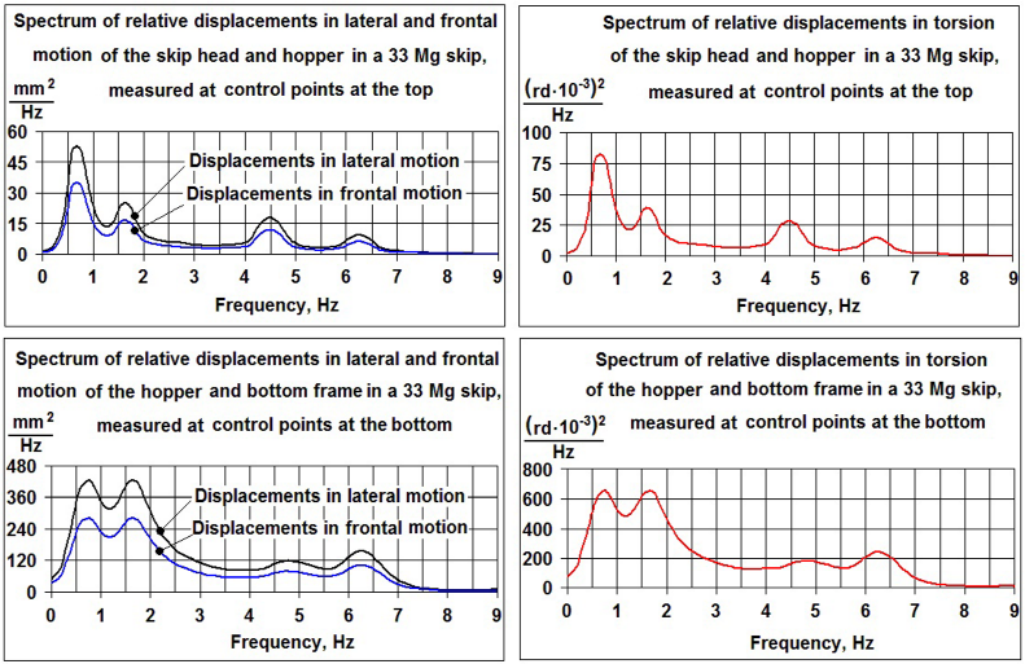

Fig. 4. Power spectral density of relative displacements in transverse vibration of a skip with the load-bearing capacity 33Mg, measured at control points at the top and bottom

Plots in Fig. 4 lead us to two important conclusions:

1) Relative displacement spectra for control points at the top and at the bottom reveal local peaks (maximums) corresponding to frequencies being the resonance frequencies of trans-verse vibrations of the investigated skip. That indicates that the skip' transverse vibrations are ex-perienced by the linear and stationary elastic-mass system and that they are induced by ran-dom misalignment of the guiding tracks in the shaft, leading to deformations the roller guide elements due to their lateral and frontal movements of a skip incorporating three major mass components connected with elastic rods replacing the upper and lower segments of pull rods.
2) Each of the three relative displacement spectra mentioned above (obtained at the upper and bottom control points): relative displacements in the lateral motion, relative frontal displa-cements and relative displacements in torsion yield comparable values. This sug-

gests that each upper and lower segment of the pull rod in the skip, exhibits a variable strain due to transverse vibrations of the skip's major mass components. This strain is also associated with the pull rod being simultaneously bent in the lateral and in frontal direction and due to torsion as well as tension to which it may be subjected.

A thorough study of main assumptions underlying the previously published equations governing the skip transverse vibration (Płachno, 1989; Tejszerska, 1993; Wolny & Matachowski, 2010) reveals that these assumptions are in line with the first of the above conclusions only. As regards the other one, they tend to neglect the effects of torsional and longitudinal stiffness of pull rod segments.

Further research (Płachno et al., 2007-2015) established that this influence is essential, therefore the relevant assumptions need to be modified accordingly and the new calculation procedure is suggested to obtain the stiffness of load-bearing pull rods in the skip. The procedure is shown in the graphic format in Fig 5 and its mathematical representation is given by Eq. (3)÷(7).

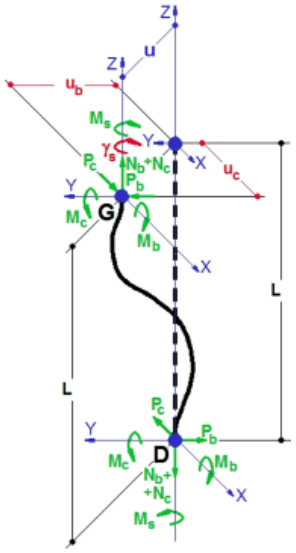

Fig. 5. Graphic representation of the procedure for calculating lateral stiffness of the skip's pull rod segments

Fig. 5 shows a pull rod spatially deformed by forces N_b, N_c, P_b, P_c and the moments of force M_b, M_s, M_c applied at the both ends (G and D), corresponding to points where the pull rods are attached to the skip head and the hopper (upper segments) or to the hopper and the lower frame (bottom segments). These forces and moments give rise to lateral displacements u_b, frontal displacements u_c and displacements in torsion γ_s of the rod end point G with respect to its end point D. Each of them corresponds to instantaneous displacements experienced by the main mass components in the investigated skip, between the control points at the top and at the bottom, at the same time the whole rod is experiencing the lengthening of the ur causing the distance. Accordingly, the forces and moments applied to the rod as shown in Fig. 5 are defined as:

P_b, P_c – forces inducing the displacements u_b, u_c;

M_b, M_c – moments acting such that the angular displacements of the rod endpoint G with respect to its endpoint D – (in the planes XZ, YZ) – are equal to zero;

M_s – moment inducing the displacement in torsion γ_s;
N_b, N_c – axial forces acting in the rod such that the distance between its endpoints G and D is independent of applied loads;

The mathematical procedure for calculating the lateral stiffness coefficients of the skip's pull rod segments is based on their following definitions:

$$k_{ub} = \frac{\partial^2 H(u_b,\ u_c,\ \gamma_s)}{\partial u_b^{\,2}},\ k_{uc} = \frac{\partial^2 H(u_b,\ u_c,\ \gamma_s)}{\partial u_c^{\,2}},\ k_{\gamma s} = \frac{\partial^2 H(u_b,\ u_c,\ \gamma_s)}{\partial \gamma_s^{\,2}} \tag{3}$$

where:
k_{ub}, k_{uc}, k_{ur}, $k_{\gamma s}$ — lateral stiffness of the upper or lower pull rod segments, respectively for bending in lateral and frontal motion and in torsion;
$H(u_b, u_c, u_r, \gamma_s)$ — elastic energy accumulated in the investigated pull rod segments whilst its end-points D and G get displaced with respect to one another by u_b, u_c, γ_s, and the distance L of these points will not change.
Elastic energy $H(u_b, u_c, u_r, \gamma_s)$ is formulated as the sum of four components:

$$H(u_b,\ u_c,\ \gamma_s) = \frac{6 \cdot E}{L^3}\left[\begin{array}{l} J_b \cdot u_b^{\,2} + J_c \cdot u_c^{\,2} + 0{,}021 \cdot F \cdot \left(\ u_b^{\,2} + u_c^{\,2}\right)^2 + \\ +0{,}032 \cdot J_s \cdot L^2 \cdot \gamma_s^{\,2} \end{array}\right] \tag{4}$$

all of which are described mathematically using the underlying dependencies applied energetic methods of calculating the displacement of rods (Lisowski & Siemieniec, 1973; Niezgodziński, 1979; Wolny, 2008) and the following signs:
E, G – modulus of elasticity of rod material, respectively Young's modulus, Kirchhoff 's, Pa;
F – cross-section area of the investigated pull rod segment, m^2;
J_b, J_c – inertia moments of the cross-section F with respect to its neutral axes for bending of the investigated pull rod segment in the lateral and frontal motion, respectively, m^4;
J_s – equivalent moment of inertia of the cross section F in free torsion, m^4;
L – as indicated in Fig. 5, m;

If we take into account that between the elongation u_r and the displacements u_b, u_c there is a relation:

$$(L + u_r)^2 = L^2 + u_b^2 + u_c^2$$

then expression (4) can be represented as:

$$H(u_b, u_c, u_r, \gamma_s) = H(u_b, u_c, \gamma_s) = \frac{6 \cdot EJ_b}{L^3} \cdot u_b^2 + \frac{6 \cdot EJ_c}{L^3} \cdot u_c^2 + \\ + \frac{EF}{2} \cdot L^2 \cdot \left(\sqrt{1 + \frac{u_b^2 + u_c^2}{L^2}} - 1\right)^2 + \frac{G \cdot J_s}{2 \cdot L} \gamma_s^2$$

and then, after considering that:

$$\frac{u_b^2+u_c^2}{L^2}<<1 \Rightarrow \sqrt{1+\frac{u_b^2+u_c^2}{L^2}} \approx 1+0{,}5\frac{u_b^2+u_c^2}{L^2} \Rightarrow u_r \approx \frac{u_b^2+u_c^2}{2\cdot L}$$

is obtained for the expression (4):

$$u_{beg} \approx 22 \text{ mm}, \quad u_{ceg} \approx 18 \text{ mm}, \quad u_{bed} \approx 79 \text{ mm}, \quad u_{ced} \approx 65 \text{ mm} \tag{5}$$

The formula (5) contains a term expressing geometric nonlinearity of the rod shown in Fig. 5 because the linearization procedure is applied (Bogusz et al., 1974) utilising measurement data (Płachno et al. 2007÷2015) showing, that in the case of rods of rectangular cross-section gxh ($g < h$), the maxi-mum amplitude $u_{b\max}$ displacements u_b and maximum amplitude $u_{c\max}$ displacements u_c satisfy the conditions:

$$k_{ubg} = \frac{12\cdot E\cdot J_{bg}}{L_g{}^3} + \frac{0{,}25\cdot E\cdot F_g}{L_g{}^3}\cdot\left(\frac{u_{beg}}{10^3}\right)^2,$$

$$k_{ucg} = \frac{12\cdot E\cdot J_c}{L_g{}^3} + \frac{0{,}25\cdot E\cdot F_g}{L_g{}^3}\cdot\left(\frac{u_{ceg}}{10^3}\right)^2,$$

$$k_{\gamma sg} = 0{,}384\cdot\frac{E\cdot J_{sg}}{L_g}. \tag{6}$$

On this basis and assuming that in the case of steel rods $G \approx 0{,}4$ E, it was obtained by the formulas (3):

$$k_{ubd} = \frac{12\cdot E\cdot J_{bd}}{L_d{}^3} + \frac{0{,}25\cdot E\cdot F_d}{L_d{}^3}\cdot\left(\frac{u_{bed}}{10^3}\right)^2,$$

$$k_{ucd} = \frac{12\cdot E\cdot J_{cd}}{L_d{}^3} + \frac{0{,}25\cdot E\cdot F_d}{L_d{}^3}\cdot\left(\frac{u_{ced}}{10^3}\right)^2,$$

$$k_{\gamma sd} = 0{,}384\cdot\frac{E\cdot J_{sd}}{L_d}. \tag{7}$$

When formulas (7) are compared with formulas expressing the lateral stiffness of pull rod segments published to date (Płachno, 1989; Tejszerska, 1993, Wolny & Matachowski, 2010), it is reasonable to apply the new calculation procedure outlined above to derive the modified equations governing the skip transverse vibration and to verify thus modified equations against the measurement data compiled in Fig. 4. The results are summarised in further sections of this study.

3. Equations governing the skip's transverse vibration due to misalignment of the guiding tracks in the hoisting shaft based on modified assumptions

Relevant equations were derived for the physical model of the system, shown schematically in Fig. 6. There are three non-deformable geometric figures under load, the total number of applied

loads being 68. These geometric figures are projections of the skip's major mass components: the skip head, the hopper and the bottom frame, underpinned by the following assumptions:

- dimensions and point C on each of the geometric figures in Fig. 6 express the dimensions and the centre of mass of the major skip's component represented by this figure;
- vertical dimensions of the skip head and bottom frame are negligibly small in relation to the sum of the skip hopper's dimensions c and d;
- forces and moments applied to the figures in Fig. 6 correspond to active and passive loads ex-perienced by the skip's major mass components in the course of its travel in the shaft; active im-posed loads involve dynamic forces induced by misalignment of the tracks guiding and inter-actions with roller guides, frontal and lateral; whilst passive loads involve forces and moments of inertia, friction and elastic resistance sustained by each of the skip's major mass component.

Further assumptions underlying the model shown in Fig. 6 are:

1. Displacements due to vibration of each geometric figure shown in Fig. 6 at points designated as 1, 2, 3, 4, 5, 6 satisfy the following equations:

- for skip head:

$$\begin{aligned} &U_{b1g} = U_{b2g} = Y_g - \Gamma_g \cdot s, \\ &U_{b3g} = U_{b4g} = Y_g + \Gamma_g \cdot s, \quad U_{b5g} = U_{b6g} = Y_g, \\ &U_{c1g} = U_{c3g} = U_{c5g} = X_g - \Gamma_g \cdot 0,5 \cdot b, \\ &U_{c2g} = U_{c4g} = U_{c6g} = X_g + \Gamma_g \cdot 0,5 \cdot b \end{aligned} \tag{8}$$

where:

$U_{b1g} \div U_{b6g}$, $U_{c1g} \div U_{c6g}$ – displacements in skip head vibrations at points 1÷6, in lateral and frontal motion, respectively;

X_g, Y_g, G_g – displacements in translational and angular vibration of the skip head, respectively;

b, s – dimensions as indicated in Fig. 6;

- for the hopper's upper edge:

$$\begin{aligned} &U_{b1zg} = U_{b2zg} = Y_z - \Gamma_z \cdot s - \Phi_z \cdot c, \\ &U_{b3zg} = U_{b4zg} = Y_z + \Gamma_z \cdot s - \Phi_z \cdot c, \quad U_{b5g} = U_{b6g} = Y_z - \Phi_z \cdot c, \\ &U_{c1zg} = U_{c3zg} = U_{c5zg} = X_z - \Gamma_z \cdot 0,5 \cdot b - B_z \cdot c, \\ &U_{c2zg} = U_{c4zg} = U_{c6zg} = X_z + \Gamma_z \cdot 0,5 \cdot b - B_z \cdot c \end{aligned} \tag{9}$$

where:

$U_{b1zg} \div U_{b6zg}$, $U_{c1zg} \div U_{c6zg}$ – displacements induced by hopper vibration, registered at points 1÷6 on its upper edges for the lateral and frontal motion, respectively;

X_z, Y_z, B_z, F_z, G_z – displacements in translational and angular vibration, respectively;

c – dimension as indicated in Fig. 6;

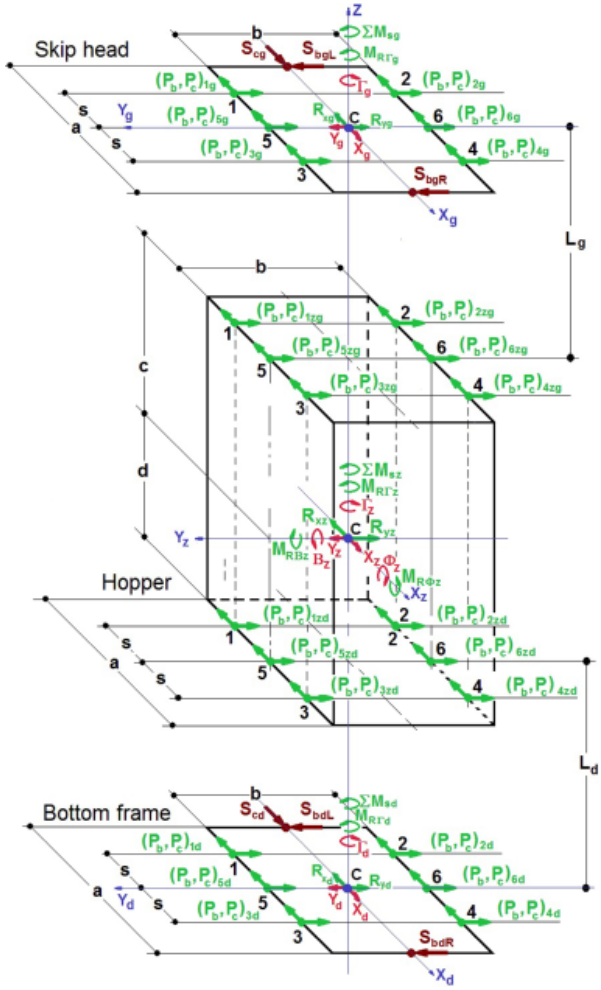

Fig. 6. Physical model of the skip underlying the equations governing its lateral and frontal vibration, based on modified assumptions

- for the hopper's lower edge:

$$
\begin{aligned}
&U_{b1zd} = U_{b2zd} = Y_z - \Gamma_z \cdot s + \Phi_z \cdot d,\\
&U_{b3zg} = U_{b4zg} = Y_z + \Gamma_z \cdot s + \Phi_z \cdot d,\ U_{b5d} = U_{b6d} = Y_z + \Phi_z \cdot d,\\
&U_{c1zd} = U_{c3zd} = U_{c5zd} = X_z - \Gamma_z \cdot 0{,}5 \cdot b + B_z \cdot d,\\
&U_{c2zd} = U_{c4zd} = U_{c6zd} = X_z + \Gamma_z \cdot 0{,}5 \cdot b + B_z \cdot d
\end{aligned}
\tag{10}
$$

where:

$U_{b1zd} \div U_{b6zd}$, $U_{c1zd} \div U_{c6zd}$ – displacements induced by hopper vibration, registered at control points 1-6 on its lower edges for the lateral and frontal motion, respectively;

d – dimension as indicated in Fig. 6;

- for the bottom frame:

$$\begin{aligned}
&U_{b1d} = U_{b2d} = Y_d - \Gamma_d \cdot s, \\
&U_{b3d} = U_{b4d} = Y_d + \Gamma_d \cdot s, \quad U_{b5d} = U_{b6d} = Y_d, \\
&U_{c1d} = U_{c3d} = U_{c5d} = X_d - \Gamma_d \cdot 0,5 \cdot b, \\
&U_{c2d} = U_{c4d} = U_{c6d} = X_d + \Gamma_d \cdot 0,5 \cdot b
\end{aligned} \tag{11}$$

where:

$U_{b1d} \div U_{b6d}$, $U_{c1d} \div U_{c6d}$ – displacements in lower frame's vibrations registered at points 1-6, for the lateral and frontal motion, respectively;

X_d, Y_d, G_d – displacements in the lower frame's translational and angular vibration, respectively.

2. Active loads imposed on the skip head and bottom frame in Fig. 6 are designated and interpreted as follows:

S_{bg1}, S_{bdR}, S_{cg}, S_{bdL}, S_{bdR}, S_{cd} – active forces induced by the skip roller guides at the upper and on the lower are applied to the system shown in Fig. 6 at the centre point of shorter sides of the skip head and of the bottom frame, expressed by the formulas:

$$\begin{aligned}
S_{bgL} &= k_{pbg} \cdot \left[Y_{pg}(t) - Y_g + 0,5 \cdot a \cdot \Gamma_g \right], \\
S_{bgR} &= k_{pbg} \cdot \left[Y_{pg}(t) - Y_g - 0,5 \cdot a \cdot \Gamma_g \right], \\
S_{cg} &= k_{pcg} \cdot \left[X_{pg}(t) - X_g \right], \\
S_{bdL} &= k_{pbd} \cdot \left[Y_{pd}(t) - Y_d + 0,5 \cdot a \cdot \Gamma_d \right], \\
S_{bdR} &= k_{pbd} \cdot \left[Y_{pd}(t) - Y_d - 0,5 \cdot a \cdot \Gamma_d \right], \\
S_{cd} &= k_{pcd} \cdot \left[X_{pd}(t) - X_d \right]
\end{aligned} \tag{12}$$

where:

a – dimension as indicated in Fig. 6,

k_{pbg}, k_{pbd} – lateral stiffness of upper and lower roller guide, respectively;

k_{pcg}, k_{pcb} – frontal stiffness of upper and lower roller guide, respectively.

$X_{pg}(t)$, $X_{pd}(t)$, $Y_{pg}(t)$, $Y_{pd}(t)$ – random functions of time describing the effects of guide misalignment on the skip roller guides, for the frontal roller guides in the upper and on the lower position, respectively, in the frontal roller guides and in the lateral roller guides, defined by ascribing the duration time of skip travel to the results of routine measurements of guide alignment (Mining regulations, 2006);

X_g, Y_d, Y_g, Y_d – vibration of the skip's major mass components, as shown in Fig. 6.

3. Passive inertia and friction loads imposed on the skip's major mass components are applied to point C (centres of major mass) and are designated and interpreted as follows:

- R_{xg}, R_{yg}, R_{xz}, R_{yz}, R_{xd}, R_{yd} – respective passive forces applied to the centre of mass of the skip head, hopper and bottom frame, satisfying the following conditions:

$$\begin{aligned}
R_{xg} &= \ddot{X}_g \cdot m_{xg} + \dot{X}_g \cdot h_{xg}, \\
R_{yg} &= \ddot{Y}_g \cdot m_{yg} + \dot{Y}_g \cdot h_{yg},
\end{aligned}$$

$$
\begin{aligned}
R_{xz} &= \ddot{X}_z \cdot m_{xz} + \dot{X}_z \cdot h_{xz}, \\
R_{yz} &= \ddot{Y}_z \cdot m_{yz} + \dot{Y}_z \cdot h_{yz}, \\
R_{xd} &= \ddot{X}_d \cdot m_{xd} + \dot{X}_d \cdot h_{xd}, \\
R_{yd} &= \ddot{Y}_d \cdot m_{yd} + \dot{Y}_d \cdot h_{yd}
\end{aligned} \tag{13}
$$

where:

m_{xg}, m_{xz}, m_{xd}, m_{yg}, m_{yz}, m_{yd} – masses corresponding to the accelerations in vibrations X_g, X_z, X_d, Y_g, Y_z, Y_d experienced by the skip's major mass components;

h_{xg}, h_{xz}, h_{xd}, h_{yg}, h_{yz}, h_{yd} – viscous damping of vibration X_g, X_z, X_d, Y_g, Y_z, Y_d experienced by the skip's major mass components;

- M_{RBz}, M_{RFz}, M_{RBz}, M_{RBz}, M_{RBz} – passive moments applied to the centre of major mass of the skip head, hopper and bottom frame, expressed as:

$$
\begin{aligned}
M_{RBz} &= \ddot{B}_z \cdot J_{\beta z} + \dot{B}_z \cdot h_{\beta z}, \\
M_{R\Phi z} &= \ddot{\Phi}_z \cdot J_{\varphi z} + \dot{\Phi}_z \cdot h_{\varphi z}, \\
M_{R\Gamma g} &= \ddot{\Gamma}_g \cdot J_{\gamma g} + \dot{\Gamma}_g \cdot h_{\gamma g}, \\
M_{R\Gamma z} &= \ddot{\Gamma}_z \cdot J_{\gamma z} + \dot{\Gamma}_z \cdot h_{\gamma z}, \\
M_{R\Gamma d} &= \ddot{\Gamma}_d \cdot J_{\gamma d} + \dot{\Gamma}_d \cdot h_{\gamma d}
\end{aligned} \tag{14}
$$

where:

$J_{\beta z}$, $J_{\varphi z}$, $J_{\gamma g}$, $J_{\gamma z}$, $J_{\gamma d}$ – principal central inertia moments of the skip's major mass components with respect to their angular vibration B_z, F_z, Γ_g, Γ_z, Γ_d;

$h_{\beta z}$, $h_{\varphi z}$, $h_{\gamma g}$, $h_{\gamma z}$, $h_{\gamma d}$ – viscous damping of angular vibration B_z, F_z, Γ_g, Γ_z, Γ_d experienced by the skip's major mass components;

4. Passive elastic forces acting upon the skip's major mass components at points 1, 2, 3, 4, 5, 6 are defined as:

- $P_{b1g} \div P_{b6g}$, $P_{b1zg} \div P_{b6zd}$, $P_{b1zd} \div P_{b6zd}$, $P_{b1d} \div P_{b6d}$ – elastic forces, each corresponding to the force P_b imposed by the rod shown in the diagram in Fig. 5 and satisfying the following condition:

$$
\begin{aligned}
P_{big} &= -P_{bizg} = k_{ubig} \cdot \left(U_{big} - U_{bizg}\right), \\
P_{bizd} &= -P_{bid} = k_{ubid} \cdot \left(U_{bizd} - U_{bid}\right), \\
i &= 1,\ 2,\ 3,\ 4,\ 5,\ 6,
\end{aligned} \tag{15}
$$

where:

U_{big}, U_{bizg}, U_{bizd}, U_{bid} – as given by formulas (8)÷(11),

k_{ubig}, k_{ubid} – lateral stiffness of the upper and lower segment of the pull rod with the i-th attachment to the skip's major mass components, derived from Eq. (6) or Eq. (7),

- $P_{c1g} \div P_{c6g}$, $P_{c1zg} \div P_{c6zg}$, $P_{c1zd} \div P_{c6zd}$, $P_{c1d} \div P_{c6d}$ – elastic forces, each corresponding to the force P_c imposed by the rod in the diagram in Fig 5 and satisfying the following condition:

$$P_{cig} = -P_{cizg} = k_{ucig} \cdot \left(U_{cig} - U_{cizg}\right),$$
$$P_{cizd} = -P_{cid} = k_{ucid} \cdot \left(U_{cizd} - U_{cid}\right),$$
$$i = 1,\ 2,\ 3,\ 4,\ 5,\ 6\,, \tag{16}$$

where:

U_{cig}, U_{cizg}, U_{cizd}, U_{cid} – as given by formulas (8)÷(11),

k_{ucig}, k_{ucid} – frontal stiffness of the upper and lower segment of the pull rod with the i-th attachment to the skip's major mass components, derived from Eq. (6) or Eq. (7).

5. Elastic passive moments applied to points C of geometric figures in the model in Fig. 6 are defi-ned as:

ΣM_{sg}, ΣM_{sz}, ΣM_{sd} – sums of moments equivalent to the moment M_s imposed on the rod shown in diagram in Fig. 5 and satisfying the respective conditions:

$$\Sigma M_{sg} = (\Gamma_g - \Gamma_z) \cdot \sum_{i=1}^{i=6} k_{\gamma sgi}, \quad \Sigma M_{sd} = (\Gamma_d - \Gamma_z) \cdot \sum_{i=1}^{i=6} k_{\gamma sdi},$$
$$\Sigma M_{sz} = (\Gamma_z - \Gamma_g) \cdot \sum_{i=1}^{i=6} k_{\gamma sgi} + (\Gamma_z - \Gamma_g) \cdot \sum_{i=1}^{i=6} k_{\gamma sdi} \tag{17}$$

where:

Γ_g, Γ_z, Γ_d – displacements in angular vibration of the skip head, hopper and the bottom frame, as shown in the diagram in Fig. 6,

$k_{\gamma sgi}$, $k_{\gamma sdi}$ – torsional stiffness of the upper and lower segment of the pull rod with the i-th attachment to the skip's major mass components, derived from Eq. (6), or Eq. (7).

6. In physical terms, underlying the equations of the skip's transverse vibration are the balance con-ditions of all imposed passive and active loads applied to geometric figures shown in Fig. 6. These conditions are expressed by the formulas:

- for vibrations X_g, X_z, X_d of the major mass centre of the skip's head, hopper and bottom frame:

$$\ddot{X}_g \cdot m_{xg} + \dot{X}_g \cdot h_{xg} + \sum_{i=1}^{i=6} \left(P_{cig}\right) - S_{cg} = 0\,,$$
$$\ddot{X}_z \cdot m_{xz} + \dot{X}_z \cdot h_{xz} + \sum_{i=1}^{i=6} \left(P_{cizg} + P_{cizd}\right) = 0\,,$$
$$\ddot{X}_d \cdot m_{xd} + \dot{X}_d \cdot h_{xd} + \sum_{i=1}^{i=6} \left(P_{cid}\right) - S_{cd} = 0 \tag{18}$$

- for vibrations Y_g, Y_z, Y_d of the mass centre of the skip's head, hopper and bottom frame:

$$\ddot{Y}_g \cdot m_{yg} + \dot{Y}_g \cdot h_{yg} + \sum_{i=1}^{i=6} \left(P_{big}\right) - S_{bLg} - S_{bPg} = 0\,,$$

$$\ddot{Y}_z \cdot m_{yz} + \dot{Y}_z \cdot h_{yz} + \sum_{i=1}^{i=6}\left(P_{bizg} + P_{bizd}\right) = 0\,,$$

$$\ddot{Y}_d \cdot m_{yd} + \dot{Y}_d \cdot h_{yd} + \sum_{i=1}^{i=6}\left(P_{bid}\right) - S_{bLd} - S_{bPd} = 0 \tag{19}$$

- for angular vibration B_z of the skip hopper:

$$\ddot{B}_z \cdot J_{\beta z} + \dot{B}_z \cdot h_{\beta z} - c \cdot \sum_{i=1}^{i=6} P_{cizg} + d \cdot \sum_{i=1}^{i=6} P_{cizd} = 0 \tag{20}$$

- for angular vibration Φ_z of the skip hopper:

$$\ddot{\Phi}_z \cdot J_{\varphi z} + \dot{\Phi}_z \cdot h_{\varphi z} - c \cdot \sum_{i=1}^{i=6} P_{bizg} + d \cdot \sum_{i=1}^{i=6} P_{bizd} = 0 \tag{21}$$

- for angular vibration Γ_g of the skip head, Γ_z of the hopper and Γ_d of the bottom frame:

$$\begin{aligned}
&\ddot{\Gamma}_g \cdot J_{\gamma g} + \dot{\Gamma}_g \cdot h_{\gamma g} - s \cdot \sum_{i=1}^{i=2} P_{big} + s \cdot \sum_{i=3}^{i=4} P_{big} + 0{,}5 \cdot b \cdot \sum_{i=1}^{i=6} (-1)^i \cdot P_{cig} + \\
&\quad + \sum M_{sg} + 0{,}5 \cdot a \cdot (S_{bLg} - S_{bPg}) = 0, \\
&\ddot{\Gamma}_z \cdot J_{\gamma z} + \dot{\Gamma}_z \cdot h_{\gamma z} - s \cdot \sum_{i=1}^{i=2} \left(P_{bizg} + P_{bizd}\right) \\
&\quad + s \cdot \sum_{i=3}^{i=4} \left(P_{bizg} + P_{bizd}\right) + 0{,}5 \cdot b \cdot \sum_{i=1}^{i=6} (-1)^i \cdot \left(P_{cizg} + P_{cizd}\right) + \sum M_{sz} = 0, \\
&\ddot{\Gamma}_d \cdot J_{\gamma d} + \dot{\Gamma}_d \cdot h_{\gamma d} - s \cdot \sum_{i=1}^{i=2} P_{bid} + s \cdot \sum_{i=3}^{i=4} P_{bid} + 0{,}5 \cdot b \cdot \sum_{i=1}^{i=6} (-1)^i \cdot P_{cid} = \\
&\quad + \sum M_{sd} + 0{,}5 \cdot a \cdot (S_{bLd} - S_{bPd}) = 0,
\end{aligned} \tag{22}$$

Substituting Eq. (8)÷(17) into Eq. (18)÷(22) yields three uncoupled system of equations gover-ning the transverse vibration of the model shown in Fig. 6:

$$\begin{aligned}
M_x \cdot \ddot{U}_x + H_x \cdot \dot{U}_x + S_x \cdot U_x &= W_x(t)\,, \\
M_y \cdot \ddot{U}_y + H_y \cdot \dot{U}_y + S_y \cdot U_y &= W_y(t)\,, \\
M_\gamma \cdot \ddot{U}_\gamma + H_\gamma \cdot \dot{U}_\gamma + S_\gamma \cdot U_\gamma &= W_\gamma(t)
\end{aligned} \tag{23}$$

where:
U_x, U_y, U_γ – column matrices given as:

$$\begin{aligned}
U_x &= \left\{ X_g \quad X_z \quad X_d \quad B_z \right\}, \\
U_y &= \left\{ Y_g \quad Y_z \quad Y_d \quad \Phi_z \right\}, \\
U_\gamma &= \left\{ \Gamma_g \quad \Gamma_z \quad \Gamma_d \right\}
\end{aligned} \tag{24}$$

M_x, M_y, M_γ – diagonal matrices of the skip's lateral stiffness whose elements are defined as:

$$\begin{aligned} &m_{x11} = m_{xg},\ m_{x22} = m_{xz},\ m_{x33} = m_{xd},\ m_{x44} = J_{\beta z}, \\ &m_{y11} = m_{yg},\ m_{y22} = m_{yz},\ m_{y33} = m_{yd},\ m_{y44} = J_{\varphi z}, \\ &m_{\gamma 11} = J_{\gamma g},\ m_{\gamma 22} = J_{\gamma z},\ m_{\gamma 33} = J_{\gamma d} \end{aligned} \tag{25}$$

H_x, H_y, H_γ – diagonal matrices of transverse vibration damping whose elements are defined as:

$$\begin{aligned} &h_{x11} = h_{xg},\ h_{x22} = h_{xz},\ h_{x33} = h_{xd},\ h_{x44} = h_{\beta z}, \\ &h_{y11} = h_{yg},\ h_{y22} = h_{yz},\ h_{y33} = h_{yd},\ h_{y44} = h_{\varphi z}, \\ &h_{\gamma 11} = h_{\gamma g},\ h_{\gamma 22} = h_{\gamma z},\ h_{\gamma 33} = h_{\gamma d} \end{aligned} \tag{26}$$

S_x – 4×4 matrix of the skip's frontal stiffness, matrix elements s_{cij} are first derived by substituting Eq. (16) and next relevant terms from Eq. (8)÷(11) into Eq. (27), yielding:

$$\begin{aligned} &s_{c11} \cdot X_g + s_{c12} \cdot X_z + s_{c13} \cdot X_d + s_{c14} \cdot B_z = k_{pcg} \cdot X_{pg}(t) + \sum_{i=1}^{i=6} P_{cig}\ , \\ &s_{c21} \cdot X_g + s_{c22} \cdot X_z + s_{c23} \cdot X_d + s_{c24} \cdot B_z = \sum_{i=1}^{i=6} \left(P_{cizg} + P_{cizd} \right), \\ &s_{c31} \cdot X_g + s_{c32} \cdot X_z + s_{c33} \cdot X_d + s_{c34} \cdot B_z = k_{pcd} \cdot X_{pd}(t) + \sum_{i=1}^{i=6} P_{cid}\ , \\ &s_{c41} \cdot X_g + s_{c42} \cdot X_z + s_{c43} \cdot X_d + s_{c44} \cdot B_z = -c \cdot \sum_{i=1}^{i=6} P_{cizg} + d \cdot \sum_{i=1}^{i=6} P_{cizd} \end{aligned} \tag{27}$$

S_y – 4×4 matrix of the skip's stiffness in lateral motion, matrix elements s_{bij} are derived from Eq. (28) by substituting formulas from Eq. (15) and relevant terms from Eq. (8)÷(11):

$$\begin{aligned} &s_{b11} \cdot Y_g + s_{b12} \cdot Y_z + s_{b13} \cdot Y_d + s_{b44} \cdot \Phi_z = 2 \cdot k_{pbg} \cdot Y_g(t) + \sum_{i=1}^{i=6} P_{big}\ , \\ &s_{b21} \cdot Y_g + s_{b22} \cdot Y_z + s_{b23} \cdot Y_d + s_{b24} \cdot \Phi_z = \sum_{i=1}^{i=6} \left(P_{bizg} + P_{bizd} \right), \\ &s_{b31} \cdot Y_g + s_{b32} \cdot Y_z + s_{b33} \cdot Y_d + s_{b34} \cdot \Phi_z = 2 \cdot k_{pbd} \cdot Y_d(t) + \sum_{i=1}^{i=6} P_{bid}\ , \\ &s_{b41} \cdot Y_g + s_{b42} \cdot Y_z + s_{b43} \cdot Y_d + s_{b44} \cdot \Phi_z = -c \cdot \sum_{i=1}^{i=6} P_{bizg} + d \cdot \sum_{i=1}^{i=6} P_{bizd} \end{aligned} \tag{28}$$

S_γ – 3×3 matrix of skip stiffness in torsional motion, matrix elements s_{gbij} are derived from Eq. (29) by substituting first formulas from Eq. (15) and next relevant terms from Eq. (8)÷(11):

$$s_{\gamma 11}\cdot\Gamma_g + s_{\gamma 12}\cdot\Gamma_z + s_{\gamma 13}\cdot\Gamma_d = 0,5\cdot a^2\cdot k_{pbg}\cdot\Gamma_g - s\cdot\sum_{i=1}^{i=2} P_{big}$$
$$+ s\cdot\sum_{i=3}^{i=4} P_{big} + 0,5\cdot b\cdot\sum_{i=1}^{i=6}(-1)^i\cdot P_{cig} + \sum M_{sg},$$
$$s_{\gamma 21}\cdot\Gamma_g + s_{\gamma 22}\cdot\Gamma_z + s_{\gamma 23}\cdot\Gamma_d = -s\cdot\sum_{i=1}^{i=2}\left(P_{bizg} + P_{bizd}\right) +$$
$$+ s\cdot\sum_{i=3}^{i=4}\left(P_{bizg} + P_{bizd}\right) + 0,5\cdot b\cdot\sum_{i=1}^{i=6}(-1)^i\cdot\left(P_{cizg} + P_{cizg}\right) + \sum M_{sz},$$
$$s_{\gamma 31}\cdot\Gamma_g + s_{\gamma 32}\cdot\Gamma_z + s_{\gamma 33}\cdot\Gamma_d = 0,5\cdot a^2\cdot k_{pbd}\cdot\Gamma_d - s\cdot\sum_{i=1}^{i=2} P_{bid} +$$
$$+ s\cdot\sum_{i=3}^{i=4} P_{bid} + 0,5\cdot b\cdot\sum_{i=1}^{i=6}(-1)^i\cdot P_{cid} + \sum M_{sd}. \qquad (29)$$

$W_x(t)$, $W_y(t)$, $W_\gamma(t)$ – diagonal matrix of excitations inducing the skip's transverse vibration, matrix elements are given as:

- for matrix $W_x(t)$:

$$w_{x11}(t) = k_{pcg}\cdot X_{pg}(t),\ \ w_{x22}(t)\equiv 0,$$
$$w_{x33}(t) = k_{pcd}\cdot X_{pd}(t),\ \ w_{x44}(t)\equiv 0 \qquad (30)$$

- for matrix $W_y(t)$:

$$w_{y11}(t) = 2\cdot k_{pbg}\cdot Y_{pg}(t),\quad w_{y22}(t)\equiv 0,$$
$$w_{y33}(t) = 2\cdot k_{pbd}\cdot Y_{pd}(t),\ \ w_{y44}(t)\equiv 0 \qquad (31)$$

- for matrix $W_\gamma(t)$:

$$w_{\gamma 11}(t) = a\cdot k_{pbg}\cdot Y_{pg}(t),\quad w_{\gamma 22}(t)\equiv 0,$$
$$w_{\gamma 33}(t) = a\cdot k_{pbd}\cdot Y_{pd}(t) \qquad (32)$$

where: a, k_{pbg}, k_{pbd}, k_{pcg}, k_{pcd}, $X_{pg}(t)$, $X_{pd}(t)$, $Y_{pg}(t)$, $Y_{pd}(t)$ – as expressed in formula (12).

It results from the system of equations (23) show that $\{X_g X_z X_d B_z\}$ – skip vibration in frontal motion, its vibrations $\{Y_g Y_z, Y_d, \Phi_z\}$ in lateral motion and $\{\Gamma_g, \Gamma_z, \Gamma_d\}$ – skip torsional vibrations are mutually independent, which is indicative of different frequency patterns. This suggestion, however, is not corroborated by diagrams in Fig. 4 showing the spectra of relative displacements of the skip head and hopper and the hopper and the skip's bottom frame. Accordingly, thus formula-ted equations of the skip's transverse vibrations were verified against the vibration measurement data compiled in Fig. 4.

4. Verification of modified equations governing the skip's transverse vibrations

1. The key aspect of the verification procedure was to compare the frequencies corresponding to the local peaks in plots in Fig. 4 showing the spectra of relative displacements during transverse skip vibrations, measured on a real 33 Mg skip, resonance frequencies of the skip's transverse vibra-tions derived from Eq. (23). Research work carried out to date (Płachno et al., 2007-2015) re-vealed only minor damping of skips' transverse vibrations, therefore an assumption was made that resonance frequencies to be calculated will be sufficiently well approximated by natural frequencies of the skip's transverse vibrations, obtained from Eq. (23).

2. The natural frequency analysis recalls the systems of equations (23) expressed as:

- for skip vibration in forward motion $U_x = \{X_g\, X_z\, X_d\, B_z\}$:

$$M_x \cdot \ddot{U}_x + S_x \cdot U_x = 0,\ M_x = \begin{array}{|c|c|c|c|} \hline m_{x11} & 0 & 0 & 0 \\ \hline 0 & m_{x22} & 0 & 0 \\ \hline 0 & 0 & m_{x33} & 0 \\ \hline 0 & 0 & 0 & m_{x44} \\ \hline \end{array},\quad S_x = \begin{array}{|c|c|c|c|} \hline s_{c11} & s_{c12} & s_{c13} & s_{c14} \\ \hline s_{c21} & s_{c22} & s_{c23} & s_{c24} \\ \hline s_{c31} & s_{c32} & s_{c33} & s_{c34} \\ \hline s_{c41} & s_{c42} & s_{c43} & s_{c44} \\ \hline \end{array} \tag{33}$$

where:

$m_{x11}, m_{x22}, m_{x33}, m_{x44}$ – frontal inertia parameters of the investigated 33 Mg skip compiled in table 2 are derived from Eq. (25), basing on the design documentation of the skip made available by the skip owner for the purpose of the present study;

$s_{c11}, s_{c12}, ..., s_{c43}, s_{c44}$ – frontal stiffness parameters of the investigated 33 Mg skip compiled in table 3, corresponding to the construction data of this skip are contained in the Tab. 1, calcu-lated with the formulas (36) obtained from equations (27) after substituting first the formulas (16) and then the corresponding expressions from formulas (8)÷(11);

- for lateral vibration $U_y = \{Y_g\, Y_z\, Y_d\, \Phi_z\}$:

$$M_y \cdot \ddot{U}_y + S_y \cdot U_y = 0,\ M_x = \begin{array}{|c|c|c|c|} \hline m_{y11} & 0 & 0 & 0 \\ \hline 0 & m_{y22} & 0 & 0 \\ \hline 0 & 0 & m_{y33} & 0 \\ \hline 0 & 0 & 0 & m_{y44} \\ \hline \end{array},\quad S_y = \begin{array}{|c|c|c|c|} \hline s_{b11} & s_{b12} & s_{b13} & s_{b14} \\ \hline s_{b21} & s_{b22} & s_{b23} & s_{b24} \\ \hline s_{b31} & s_{b32} & s_{b33} & s_{b34} \\ \hline s_{b41} & s_{b42} & s_{b43} & s_{b44} \\ \hline \end{array} \tag{34}$$

where:

$m_{y11}, m_{y22}, m_{y33}, m_{y44}$ – lateral inertia parameters of the investigated 33 Mg skip, compiled in table 2 were derived from Eq. (25), basing on the design documentation of the skip made available by the skip owner for the purpose of the present study;

$s_{b11}, s_{b12}, ..., s_{b43}, s_{b44}$ – lateral stiffness parameters of the investigated 33Mg skip, compiled in table 4, corresponding to the construction data of this skip are contained in the Tab. 1, calcu-lated with the formulas (37) obtained from equations (28) after substituting first the formulas (15) and then the corresponding expressions from formulas (8)÷(11);

- for torsional vibrations $U_\gamma = \{\Gamma_g\ \Gamma_z\ \Gamma_d\}$:

$$M_\gamma \cdot \ddot{U}_\gamma + S_\gamma \cdot U_\gamma = 0, \quad M_\gamma = \begin{array}{|c|c|c|} \hline m_{\gamma 11} & 0 & 0 \\ \hline 0 & m_{\gamma 22} & 0 \\ \hline 0 & 0 & m_{\gamma 33} \\ \hline \end{array}, \quad S_\gamma = \begin{array}{|c|c|c|} \hline s_{\gamma 11} & s_{\gamma 12} & s_{\gamma 13} \\ \hline s_{\gamma 21} & s_{\gamma 22} & s_{\gamma 23} \\ \hline s_{\gamma 31} & s_{\gamma 32} & s_{\gamma 32} \\ \hline \end{array} \tag{35}$$

where:

$m_{\gamma 11}$, $m_{\gamma 22}$, $m_{\gamma 33}$, $m_{\gamma 44}$ – torsional inertia parameters of the investigated 33 Mg skip, compiled in table 2 are derived from Eq. (25), basing on the design documentation of the skip made available by the skip owner for the purpose of the present study;

$s_{\gamma 11}$, $s_{\gamma 12}$, ..., $s_{\gamma 43}$, $s_{\gamma 44}$ – torsional stiffness parameters of the investigated 33 Mg skip, compiled in table 5, corresponding to the construction data of this skip are contained in the Tab. 1, cal-culated with the formulas (38) obtained from equations (29) after substituting first the formulas (15)÷(17) and then the corresponding expressions from formulas (8)÷(11).

TABLE 1

Design data of a real 33 Mg skip recalled in the procedure for calculating the natural frequencies o f the skip transverse vibration

a	b	c	d	E	F_g	F_d	J_{bg}	J_{bd}	J_{cg}
m	m	m	m	Pa	m^2	m^2	m^4	m^4	m^4
3,2	1,3	3,9	2,0	$2{,}1\cdot10^{11}$	$75\cdot10^{-4}$	$54\cdot10^{-4}$	$56\cdot10^{-8}$	$41\cdot10^{-8}$	$39\cdot10^{-6}$
J_{cd}	J_{sg}	J_{sd}	k_{pbg}	k_{pbd}	k_{pcg}	k_{pcd}	L_g	L_d	s
m^4	m^4	m^4	N/m	N/m	N/m	N/m	m	m	m
$15\cdot10^{-6}$	$2\cdot10^{-6}$	$1{,}4\cdot10^{-6}$	$1{,}5\cdot10^{6}$	$1{,}5\cdot10^{6}$	$2{,}5\cdot10^{6}$	1,7	3,3	5,1	0,8

TABLE 2

Parameters expressing the skip inertia (for a real mining skip 33 Mg)

m_{x11}	m_{x12}	m_{x13}	m_{x14}	m_{y11}	m_{y22}	m_{y33}	m_{y44}	m_{g11}	m_{g22}	m_{g33}
kg	kg	kg	kgm^2	kg	kg	kg	kgm^2	kgm^2	kgm^2	kgm^2
4520	52300	3290	401900	4520	52300	3290	263600	8170	32100	5390

TABLE 3

Parameters expressing the frontal stiffness of a real mining skip 33 Mg calculated using the formulas (36) for data from Table 1

s_{c11}	s_{c12}	s_{c13}	s_{c14}	s_{c21}	s_{c22}	s_{c23}	s_{c24}
N/m	N/m	N/m	N/m	N/m	N/m	N/m	N
$13{,}5\cdot10^{6}$	$-11{,}1\cdot10^{6}$	0	$43\cdot10^{6}$	$-11{,}1\cdot10^{6}$	$12{,}2\cdot10^{6}$	$-1{,}2\cdot10^{6}$	$-41\cdot10^{6}$
s_{c31}	s_{c32}	s_{c33}	s_{c34}	s_{c41}	s_{c42}	s_{c43}	s_{c44}
N/m	N/m	N/m	N	N	N	N	N·m
0	$-1{,}2\cdot10^{6}$	$2{,}9\cdot10^{6}$	$-2{,}3\cdot10^{6}$	$43\cdot10^{6}$	$-41\cdot10^{6}$	$-2{,}3\cdot10^{6}$	$173\cdot10^{6}$

TABLE 4

Parameters expressing the lateral stiffness of a real mining skip 33 Mg calculated using the formulas (37) for data from Table 1

s_{b11}	s_{b12}	s_{b13}	s_{b14}	s_{b21}	s_{b22}	s_{b23}	s_{b24}
N/m	N/m	N/m	N/m	N/m	N/m	N/m	N
$3{,}3\cdot10^6$	$-0{,}27\cdot10^6$	0	$1{,}0\cdot10^6$	$-0{,}27\cdot10^6$	$0{,}32\cdot10^6$	$-0{,}05\cdot10^6$	$-0{,}94\cdot10^6$
s_{b31}	s_{b32}	s_{b33}	s_{b34}	s_{b41}	s_{b42}	s_{b43}	s_{b44}
N/m	N/m	N/m	N	N	N	N	N·m
0	$-0{,}05\cdot10^6$	$3{,}1\cdot10^6$	$-0{,}11\cdot10^6$	$1{,}0\cdot10^6$	$-0{,}94\cdot10^6$	$-0{,}11\cdot10^6$	$4{,}3\cdot10^6$

TABLE 5

Parameters expressing t the orsional stiffness of a real l mining skip 33 Mg calculated using the formulas (38) for data from Table 1

s_{g11}	s_{g12}	s_{g13}	s_{g21}	s_{g22}	s_{g23}	s_{g31}	s_{g32}	s_{g33}
N·m	N·m	N·m	N·m	N·m	N·m	N·m	N·m	N·m
$12{,}7\cdot10^6$	$-5{,}1\cdot10^6$	0	$-5{,}1\cdot10^6$	$5{,}7\cdot10^6$	$-0{,}62\cdot10^6$	0	$-0{,}62\cdot10^6$	8,3

3. Formulas (36) have the form:

$$s_{c11} = k_{pcg} + 4\cdot k_{ucg},\quad s_{c12} = -4\cdot k_{ucg},\quad s_{c13} = 0,\quad s_{c14} = 4\cdot c\cdot k_{ucg},$$
$$s_{c21} = s_{c12},\quad s_{c22} = 4\cdot\left(k_{ucg} + k_{ucd}\right),\quad s_{c23} = -4\cdot k_{ucd},\quad s_{c24} = -4\cdot\left(c\cdot k_{ucg} - d\cdot k_{ucd}\right)$$
$$s_{c31} = 0,\quad s_{c32} = s_{c23},\quad s_{c33} = k_{pcd} + 4\cdot k_{ucd},\quad s_{c34} = -4\cdot d\cdot k_{ucd},$$
$$s_{c41} = s_{c14},\quad s_{c42} = s_{c24},\quad s_{c43} = s_{c34},\quad s_{c44} = 4\cdot\left(c^2\cdot k_{ucg} + d^2\cdot k_{ucd}\right) \tag{36}$$

where:

c, d – as in fig. 4, the dimensions of the skip hopper having the values given in Tab. 1,

k_{pcg}, k_{pcd} – as in the formula (12), the frontal stiffness of the guide roller, respectively, of the upper and lower guide, having a value for the skip analyzed in Tab. 1,

k_{ucg}, k_{ucd} – frontal stiffness of the upper and lower segment of the pull rod, calculated from the appropriate formulas (6), (7) after substituting E, F_g, F_d, J_{cg}, J_{cd}, L_g, L_d.

4. Formulas (37) have the form:

$$s_{b11} = 2\cdot k_{pbg} + 4\cdot k_{ubg},\quad s_{b12} = -4\cdot k_{ubg},\quad s_{b13} = 0,\quad s_{b14} = 4\cdot c\cdot k_{ubg},$$
$$s_{b21} = s_{b12},\quad s_{b22} = 4\cdot\left(k_{ubg} + k_{ubd}\right),\quad s_{b23} = -4\cdot k_{ubd},\quad s_{b24} = -4\cdot\left(c\cdot k_{ubg} - d\cdot k_{ubd}\right),$$
$$s_{b31} = 0,\quad s_{b32} = s_{b23},\quad s_{b33} = 2\cdot k_{pbd} + 4\cdot k_{ubd},\quad s_{b34} = -4\cdot d\cdot k_{ubd},$$
$$s_{b41} = s_{b14},\quad s_{b42} = s_{b24},\quad s_{b43} = s_{b34},\quad s_{b44} = 4\cdot\left(c^2\cdot k_{ubg} + d^2\cdot k_{ubd}\right) \tag{37}$$

where:

c, d – as in formulas (36),

k_{pbg}, k_{pbd} – as in the formula (12), the lateral stiffness of the guide roller, respectively, of the upper and lower guide, having a value for the skip analyzed in Tab. 1,

k_{ubg}, k_{ubd} – lateral stiffness of the upper and lower segment of the pull rod, calculated from the appropriate formulas (6), (7) after substituting E, F_g, F_d, J_{bg}, J_{bd}, L_g, L_d.

5. Formulas (38) have the form:

$$
\begin{aligned}
&s_{\gamma 11} = 0,5 \cdot a^2 \cdot k_{pbg} + 4 \cdot \left[s^2 \cdot k_{ubg} + 0,25 \cdot b^2 \cdot k_{ucg} + k_{\gamma sg} \right] ,\\
&s_{\gamma 12} = -4 \left[s^2 \cdot k_{ubg} + 0,25 \cdot b^2 \cdot k_{ucg} + k_{\gamma sg} \right] , \quad s_{\gamma 13} = 0 ,\\
&s_{\gamma 21} = s_{\gamma 12} , \quad s_{\gamma 22} = 4 \cdot \left[s^2 \cdot \left(k_{ubg} + k_{ubd} \right) + 0,25 \cdot b^2 \cdot \left(k_{ucg} + k_{ucd} \right) + k_{\gamma sg} + k_{\gamma sd} \right] ,\\
&s_{\gamma 23} = -4 \cdot \left[s^2 \cdot k_{ubd} + 0,25 \cdot b^2 \cdot k_{ucd} + k_{\gamma sd} \right] ,\\
&s_{\gamma 31} = s_{\gamma 13}, \quad s_{\gamma 32} = s_{\gamma 23}, \quad s_{\gamma 33} = 0,5 \cdot a^2 \cdot k_{pbd} + 4 \cdot \left[s^2 \cdot k_{ubd} + 0,25 \cdot b^2 \cdot k_{ucd} + k_{\gamma sd} \right]
\end{aligned} \tag{38}
$$

where:

a, b, s – as in fig. 4, the dimensions of the skip hopper having the values given in Tab. 1

k_{pbg}, k_{pbd} – as in the formula (37),

k_{ubg}, k_{ubd}, k_{ucg}, k_{ucg} – as in the formulas (36) i (37),

k_{gsg}, k_{gsd} – torsional stiffness of the upper and lower segment of the pull rod, calculated from the appropriate formulas (6), (7) after substituting E, F_g, F_d, J_{sg}, J_{sd}, L_g, L_d.

6. By zeroing the coefficients of natural vibration amplitudes (Bogusz et al., 1974), natural frequen-cies of the skip's transverse vibration can be derived accordingly:

- for frontal vibration

$$
\begin{vmatrix}
s_{c11} - 4\pi^2 \cdot f_x{}^2 \cdot m_{x11} & s_{c12} & s_{c13} & s_{c14} \\
s_{c21} & s_{c22} - 4\pi^2 \cdot f_x{}^2 \cdot m_{x22} & s_{c23} & s_{c24} \\
s_{c31} & s_{c32} & s_{c33} - 4\pi^2 \cdot f_x{}^2 \cdot m_{x33} & s_{c34} \\
s_{c41} & s_{c42} & s_{c43} & s_{c44} - 4\pi^2 \cdot f_x{}^2 \cdot m_{x44}
\end{vmatrix} = 0 \tag{39}
$$

- for lateral vibration

$$
\begin{vmatrix}
s_{b11} - 4\pi^2 \cdot f_y{}^2 \cdot m_{y11} & s_{b12} & s_{b13} & s_{b14} \\
s_{b21} & s_{b22} - 4\pi^2 \cdot f_y{}^2 \cdot m_{y22} & s_{b23} & s_{b24} \\
s_{b31} & s_{b32} & s_{b33} - 4\pi^2 \cdot f_y{}^2 \cdot m_{x33} & s_{b34} \\
s_{b41} & s_{b42} & s_{b43} & s_{b44} - 4\pi^2 \cdot f_y{}^2 \cdot m_{y44}
\end{vmatrix} = 0 \tag{40}
$$

- for torsional vibration

$$
\begin{vmatrix}
s_{\gamma 11} - 4\pi^2 \cdot f_\gamma{}^2 \cdot m_{\gamma 11} & s_{\gamma 12} & s_{\gamma 13} \\
s_{\gamma 21} & s_{\gamma 22} - 4\pi^2 \cdot f_\gamma \cdot m_{\gamma 22} & s_{\gamma 33} \\
s_{\gamma 31} & s_{\gamma 32} & s_{\gamma 33} - 4\pi^2 \cdot f_\gamma \cdot m_{\gamma 33}
\end{vmatrix} = 0 \tag{41}
$$

where f_x, f_y, f_γ – calculated natural frequencies.

7. To evaluate the effectiveness of the applied verification procedure, frequencies being compared are summarised in Table 6, where the frequencies corresponding to local peaks in the power spectra density in Fig. 4 are expressed as lower frequency f_d, midpoint frequency f_m and upper frequency f_g for each peak – related interval, whilst natural frequencies f_x, f_y, f_γ are derived from Eq. (39)÷(41).

TABLE 6

Measured and predicted frequencies of transverse vibration of a 33 Mg skip

Frequencies associated with local peaks in the power spectra of transverse vibration, measured for a 33 Mg skip, Hz											
First peak interval			Second peak interval			Third peak interval			Fourth peak interval		
f_{d1}	f_{m1}	f_{g1}	f_{d2}	f_{m2}	f_{g2}	f_{d3}	f_{m3}	f_{g3}	f_{d4}	f_{m4}	f_{g4}
0,3	0,7	1,1	1,1	1,6	2,1	3,8	4,7	5,6	5,6	6,3	7,0
Natural frequencies of frontal vibration of a 33 Mg skip derived from Eq. (39), Hz											
$f_{x1} = 0{,}71$			$f_{x2} = 1{,}58$			$f_{x3} = 4{,}73$			there is no		
Natural frequencies of lateral vibration for a 33 Mg skip derived from Eq. (40), Hz											
$f_{y2} = 0{,}69$			there is no			$f_{y3} = 4{,}29$, $f_{y3} = 4{,}85$			there is no		
Natural frequencies of torsional vibration for a 33 Mg skip derived from Eq. (41), Hz											
there is no			$f_{g1} = 1{,}66$			there is no			$f_{g2} = 6{,}25, f_{g3} = 6{,}42$		

8. Table 6 confirms the adequacy of the applied verification procedure because ten out of eleven natural frequencies obtained from Eq. (33)÷(35) for a real 33 Mg skip agree well with the midpoint frequencies within the local peak intervals in the power spectrum pattern for the skip transverse vibration. Specifically:

$$f_{x1} \cong f_{m1},\ f_{x2} \cong f_{m2},\ f_{x3} \cong f_{m3},\ f_{y2} \cong f_{m1},$$
$$0{,}5 \cdot \left(f_{y3} + f_{y4}\right) \cong f_{m3},\ f_{\gamma 1} \cong f_{m2},\ 0{,}5 \cdot \left(f_{\gamma 2} + f_{\gamma 3}\right) \cong f_{m4}$$

whereas the two remaining frequencies: f_{x4} and f_{y1} fall outside the interval $[f_{d1}, f_{g4}]$ in which the power spectra, as shown in Fig. 4, have significant values. Besides, frequency values derived from mutually independent systems of equations (33)-(35) are in good agreement:

$$f_{x1} \approx f_{y2},\quad f_{x2} \approx f_{\gamma 1},\quad f_{x3} \approx 0{,}5 \cdot \left(f_{\gamma 2} + f_{\gamma 3}\right)$$

This is the explanation for the fact that all power spectra of the investigated vibrations of real skip – shown in Fig 4 – reveal four local peaks involving the same frequencies.

4. Conclusions

1. Development of the mathematical model of transverse vibration of a high-capacity mining skip due to misalignment of the guiding tracks in the shaft remains a major challenge for researchers as well as the design engineers, whilst practitioners responsible for safety of hoisting operations in mines await the solution that could be used to develop a reliable methodology for

computing the fatigue endurance of skip installations being designed. So far fatigue endurance calculations have not been performed and that is why a large number of high-capacity skips incur fatigue damage having completed a smaller number of duty cycles than planned.

2. Mathematical models proposed to date were regarded unsatisfactory by the engineering com-munity, and their stance can be further justified by transverse vibration measurement data sum-marised in this study, the measurements being taken on eight high-capacity skips. Measure-ment data clearly indicate that model versions presented so far are incomplete and require further modifications, both in terms of their underlying assumptions and the involved equations, and such modification is proposed in this study. As regards the underlying assumptions, a new algorithm is proposed for calculating the transverse stiffness of particular segments of the pull rods, whilst in terms of the model itself, the modified equations are derived that govern the skip frontal, lateral and torsional vibrations. These equations were positively verified against the power spectrum patterns of such vibrations measured for a mining skip with the load-bearing capacity 33 Mg, operated in a colliery in Poland.

References

Bąk E., Myszor Z., 1999. *Utrzymanie poziomu bezpieczeństwa zespołów szybowych w czasie eksploatacji z wykorzystaniem technologii spawania i specjalnych metod łączenia*. Wydawnictwo AGH, Kraków, Zeszyty Naukowo-Techniczne KTL, 15, 193-200.

Bogusz W. i in., 1974. *Drgania i szumy*. Wydawnictwa Geologiczne, Warszawa, 124-149.

Brodziński S., Śmiałek Z., 1993. *Wybrane zagadnienia bezpieczeństwa wyciągów szybowych*. Bezpieczeństwo i Ochrona Środowiska w Górnictwie, 26, 21-26.

Fuchs D., Noeller H., 1998. *Untersuchungen an Haupttraggliedern hochbeanspruchter Fördermittel.* Sonderabdruck aus Glückauf 124 nr 9, 512-514.

Kędziora A., 1983. *Eksploatacja szybowych urządzeń wyciągowych*. Wydawnictwo „Śląsk", Katowice, 82-91.

Lisowski A., Siemieniec A., 1973. *Wytrzymałość materiałów*. PWN, Warszawa-Kraków, 111-174.

Matachowski F., 2011. *Opracowanie kryteriów projektowania wybranych elementów nośnych naczynia wyciągowego*. Unpublished doctoral thesis made at the UST-AGH, Kraków, 42-91.

Niezgodziński M.E., Niezgodzinski T., 1979. *Wytrzymałość materiałów*. PWN.75-90.

Płachno M. et al., 1984-1988. *Badania drgań poprzecznych naczyń wyciągowych eksploatowanych w szybach KWK Grodziec, KWK Sosnowiec, KWK ZMP, KWK Rydułtowy, KWK Marcel, KWK Bolesław Śmiały, ZG Sieroszowice, ZG Rudna*. Unpublished test reports carried out under the direction of M. Płachno.

Płachno M., 1988. *Zagadnienie wpływu dynamiki prowadzenia szybowego na bezpieczeństwo eksploatacji naczyń wyciągowych.* Bezpieczeństwo Pracy w Górnictwie, 4, 26-28.

Płachno M., 1989. *Zagadnienie drgań poprzecznych naczyń wyciągowych*. Zeszyty Naukowe Politechniki Śląskiej, Górnictwo, 180, 147-159.

Płachno M., Rosner Z., 1997 *Możliwości wczesnego wykrywania procesów zmęczeniowych w cięgnach naczyń wyciągów górniczych*. Bezpieczeństwo Pracy i Ochrona Środowiska w Górnictwie. Wydanie Specjalne, 241-246.

Płachno M., 1999a. *Możliwości oceny bezpieczeństwa naczyń i zbrojenia szybów metodą analizy drgań poprzecznych, zmierzonych przy naczyniach*. Wydawnictwo AGH, Kraków, Zeszyty Naukowo-Techniczne KTL, 15, 71-80.

Płachno M., 1999b. *Metoda pomiaru i analizy drgań poprzecznych naczyń wyciągowych przydatna do wyznaczania rzeczywistych obciążeń tych naczyń oraz zbrojenia szybowego*. Wydawnictwo AGH, Kraków, Zeszyty Naukowo--Techniczne KTL, 15, 81-90.

Płachno M., 2007. *Metoda dynamiczna badań stanu zmienności naprężeń w cięgnach naczyń wyciągowych powodowanego nierównościami torów prowadzenia*. Article in monograph „Transport szybowy 2007“. Wydawnictwo KOMAG, Gliwice, II, 51-60.

Płachno M. et al., 2007÷2015. *Badania stanu zmienności naprężeń powodowanego w cięgnach nośnych naczyń wyciągowych nierównościami torów prowadzenia*. Unpublished test reports carried out under the direction of M. Płachno.

Przepisy Górnicze, 2006. *Rozporządzenie Min. Gosp. z dnia 9 czerwca 2006 r. zmieniające rozporządzenie w sprawie bezpieczeństwa i higieny pracy, prowadzenia ruchu oraz specjalistycznego zabezpieczenia przeciwpożarowego w podziemnych zakładach górniczych*. Dz. U. nr 124 z 2006 r. poz. 863.

Tejszerska D., 1993. *Modelowanie drgań poprzecznych naczynia wydobywczego*. Zeszyty Naukowe Politechniki Śląskiej, Mechanika, 113, 86-95.

Tejszerska D., 1995. *Modelowanie sprzężonych drgań poprzeczno-wzdłużnych układu wyciągowego*. Zeszyty Naukowe Politechniki Śląskiej, Mechanika 124, 30-46.

Tejszerska D. et al., 2001. *Analiza częstotliwościowa układu wyciągowego.* Wydawnictwo AGH, Kraków, Zeszyty Naukowo-Techniczne KTL, 22, 75-80.

Tejszerska D., 2002. *Modelowanie i optymalizacja dynamiki wyciągów szybowych*. Monograph. Wydawnictwa Politechniki Śląskiej, Gliwice, 38-49.

Wolny S., Siemieniec A., 2008.*Wytrzymałość materiałów*. Wydawnictwa AGH, I, 163-167.

Wolny S., Bella V., 2005. *Analiza przyczyn pękania elementów nośnych naczyń wyciągowych*. Transport Przemysłowy, 3, 53-56.

Wolny S., 2009. *Assessment of Hoist Control to Ensure Conveyance Guiding*. Archives of Mining Sciences 54, 463-492.

Wolny S., Matachowski F., 2010. *Operating loads of the shaft steelwork-conveyance system due to random irregularities of the guiding string*s. Archives of Mining Sciences, 55, 334-356

Wolny S., Matachowski F., 2011: *Analysis of Loads in the conveyance-shaft steelwork system in the context of certain simplifying assumptions*. Archives of mining Sciences, 56, 305-328.